

Global Tracking Passivity-based PI Control of Bilinear Systems and its Application to the Boost and Modular Multilevel Converters

R. Cisneros *

M. Pirro **G. Bergna ***R. Ortega *G. Ippoliti **M. Molinas ***

* Laboratoire de Signaux et Systèmes, Supélec, 91190 Gif-sur-Yvette,
France (e-mail: cisneros[ortega]@lss.supelec.fr)

** Dipartimento Ingegneria dell'Informazione, Università Politecnica
delle Marche, 60121 Ancona, Italia
(e-mail:m.pirro[gianluca.ippoliti]@univpm.it)

*** Norwegian University of Science and Technology, 7491 Trondheim,
Norway (e-mail: gilbert.bergnadiaz@supelec.fr,
marta.molinas@ntnu.no)

Abstract: This paper deals with the problem of trajectory tracking of a class of bilinear systems with time-varying measurable disturbance, namely, systems of the form $\dot{x}(t) = [A + \sum_i u_i(t)B_i]x(t) + d(t)$. A set of matrices $\{A, B_i\}$ has been identified, via a linear matrix inequality, for which it is possible to ensure global tracking of (admissible, differentiable) trajectories with a simple linear time-varying PI controller. Instrumental to establish the result is the construction of an output signal with respect to which the incremental model is passive. The result is applied to the boost and the modular multilevel converter for which experimental results are given.

Keywords: Bilinear systems, global tracking, passivity, power converters, power factor compensation, modular multilevel converter.

1. INTRODUCTION

Bilinear systems are a class of nonlinear systems that describe a broad variety of physical and biological phenomena Mohler (2003) serving, sometimes, as a natural simplification of more complex nonlinear systems. There is an amount of literature devoted to the study of the intrinsic properties or to stabilization of equilibrium points for these systems, see for example Elliot (2009). However, to the best of our knowledge, there is no general result for the design of controllers that ensure *global tracking* of (admissible, differentiable) trajectories.

The main objective of this paper is to provide a theoretical framework—based on the property of passivity of the incremental model—to establish such a result. Our motivation to pursue a passivity framework is twofold, on one hand, it encompasses a large class of physical systems. On the other hand, it naturally leads to the design of PI controllers, which are known to be simple, robust and widely accepted by practitioners. Our main result is an extension, to the problem of tracking trajectories, of Jayawardhana et al. (2007); Sanders and Verghese (1992) that treat the regulation case. See also Castaños et al. (2009) for its application to PI stabilization of RLC circuits and Hernandez-Gomez et al. (2010) where the result is used in power converters.

An important motivation for our research is the derivation of simple tracking controllers for power converters. In classical applications of power converters the control objective is to *regulate* the output voltage (or current) around some constant desired value. Modern applications, on the other hand, are concerned with the more demanding specification of ensuring an effective transfer of power between the sources and the loads—an objective that translates into the task of *tracking time-varying references*.

In the paper our theoretical result has been illustrated with the application to two important problems arising in power electronic systems. The first one is the problem of Power Factor Compensation (PFC), which arises in renewable energy and motor drive systems with stringent specifications on efficiency, harmonic distortion and voltage regulation Fadili et al. (2012); Hussain et al. (2011); Mather and Maksimovic (2011); Cimini et al. (2013). The second problem is related to High Voltage Direct Current (HVDC) transmission, which has recently attracted a lot of interest Flourentzou et al. (2009); Bahrman and Johnson (2007); Ahmed et al. (2011); Zonetti et al. (2014). HVDC transmission consists of a grid comprising mostly DC lines that integrates, via voltage source converters, renewable energies from distant locations. One of the most promising candidates to integrate the topology of the grid is the Modular Multilevel Converter (MMC) Glinka and Marquardt (2003), which has several advantages with re-

spect to its predecessors, such as high modularity, scalability and lower losses. In view of its complicated topology and operating regimes, controlling the MMC is no simple task. In particular, to exploit the full potential of the MMC it seems to be necessary to develop control strategies for the system operating in the rotating (*abc*) frame Bergna et al. (2013), this is contrast with the classical strategies developed in fixed (*dq0*) frames Tu et al. (2011); Bergna et al. (2012). This situation leads to a tracking problem instead of the typical regulation one. The tracking problem of bilinear systems has been addressed within the context of switched power converters. In Olm et al. (2011) a methodology to track periodic signals for non-minimum phase boost converters based on a stable inversion of the internal dynamics taking the normal form of an Abel ordinary differential equation was presented—see also Fossas and Olm (2009). There are also schemes involving sliding mode control, for example Fossas and Olm (1994); Biel et al. (2004), and references therein. In Meza et al. (2008) the well-known passivity property of Sanders and Verghese (1992) is used to address an “approximate” tracking problem for an inverter connected to a photovoltaic solar panel. A similar framework was studied in Meza et al. (2012).

The remainder of this paper is organized as follows. Problem formulation is presented in Section 2. Our main theoretical result is contained in Section 3, where a linear matrix inequality (LMI) condition is imposed to solve the tracking problem—invoking passivity theory. Section 4 is devoted to the synthesis of a PI controller that ensures tracking trajectory, under some suitable detectability assumptions. The result is applied in Sections 5 and 6 to the two power electronic applications mentioned above. Simulations and experimental results are included in these two sections. Finally, conclusions in Section 7 complete the paper. A preliminary version of this paper was reported in Cisneros et al. (2015)

2. GLOBAL TRACKING PROBLEM

Consider the bilinear system

$$\dot{x}(t) = Ax(t) + d(t) + \sum_{i=1}^m u_i(t)B_i x(t) \quad (1)$$

where¹ $x \in \mathbb{R}^n$, $d \in \mathbb{R}^n$ are the state and the (measurable) disturbance vector, respectively, $u \in \mathbb{R}^m$, $m \leq n$, is the control vector, and $A \in \mathbb{R}^{n \times n}$, $B_i \in \mathbb{R}^{n \times n}$ are real constant matrices.

We will say that a function $x_* : \mathbb{R}_+ \rightarrow \mathbb{R}^n$ is an *admissible trajectory* of (1), if it is differentiable, bounded and verifies

$$\dot{x}_* = Ax_* + d + \sum_{i=1}^m u_i^* B_i x_* \quad (2)$$

for some bounded control signal $u_* : \mathbb{R}_+ \rightarrow \mathbb{R}^m$.

The global tracking problem is to find, if possible, a dynamic state-feedback controller of the form

$$\dot{z} = F(x, x_*, u_*) \quad (3)$$

$$u = H(x, x_*, u_*), \quad (4)$$

¹ For brevity, in the sequel the time argument is omitted from all signals.

where $F : \mathbb{R}^n \times \mathbb{R}^n \times \mathbb{R}^m \rightarrow \mathbb{R}^q$, $q \in \mathbb{Z}_+$, and $H : \mathbb{R}^n \times \mathbb{R}^n \times \mathbb{R}^m \rightarrow \mathbb{R}^m$, such that all signals remain bounded and

$$\lim_{t \rightarrow \infty} [x(t) - x_*(t)] = 0, \quad (5)$$

for all initial conditions $(x(0), z(0)) \in \mathbb{R}^n \times \mathbb{R}^q$ and all admissible trajectories.

In this paper a set of matrices $\{A, B_i\}$ has been characterized for which it is possible to solve the global tracking problem with a simple *linear time-varying PI controller*. The class is identified via the following LMI.

Assumption 1. $\exists P \in \mathbb{R}^{n \times n}$ such that

$$P = P^\top > 0 \quad (6)$$

$$\text{sym}(PA) \leq 0 \quad (7)$$

$$\text{sym}(PB_i) = 0, \quad (8)$$

where the operator $\text{sym} : \mathbb{R}^{n \times n} \rightarrow \mathbb{R}^{n \times n}$ computes the symmetric part of the matrix, that is

$$\text{sym}(PA) = \frac{1}{2}(PA + A^\top P).$$

To simplify the notation in the sequel the *positive semidefinite* matrix has been defined

$$Q := -\text{sym}(PA). \quad (9)$$

3. PASSIVITY OF THE BILINEAR INCREMENTAL MODEL

Instrumental to establish the main result of the paper is the following lemma.

Lemma 1. Consider the system (1) verifying the LMI of Assumption 1 and an admissible trajectory x_* . Define the incremental signals

$$(\tilde{\cdot}) := (\cdot) - (\cdot)_*,$$

and the m -dimensional output function

$$y := \mathcal{C}(x_*)x \quad (10)$$

where the map $\mathcal{C} : \mathbb{R}^n \rightarrow \mathbb{R}^{m \times n}$ is defined as

$$\mathcal{C}(x_*) := \begin{bmatrix} x_*^\top B_1^\top \\ \vdots \\ x_*^\top B_m^\top \end{bmatrix} P. \quad (11)$$

The operator $\tilde{u} \mapsto y$ is *passive* with storage function

$$V(\tilde{x}) := \frac{1}{2}\tilde{x}^\top P\tilde{x}. \quad (12)$$

Hence, it verifies the dissipation inequality

$$\dot{V} \leq \tilde{u}^\top y.$$

Proof. Combining (1) and (2) yields

$$\dot{\tilde{x}} = (A + \sum_{i=1}^m u_i B_i)\tilde{x} + \sum_{i=1}^m \tilde{u}_i B_i x_*. \quad (13)$$

Now, the time derivative of the storage function (12) along the trajectories of (13) is

$$\begin{aligned}
\dot{V}(\tilde{x}) &= \tilde{x}^\top P \left[(A + \sum_{i=1}^m u_i B_i) \tilde{x} + \sum_{i=1}^m \tilde{u}_i B_i x_* \right] \\
&= -\tilde{x}^\top Q \tilde{x} + \sum_{i=1}^m \tilde{u}_i \tilde{x}^\top P B_i x_* \\
&\leq \sum_{i=1}^m \tilde{u}_i \tilde{x}^\top P B_i x_* \\
&= \sum_{i=1}^m \tilde{u}_i x_*^\top P B_i x_* \\
&= y^\top \tilde{u},
\end{aligned}$$

where (8) of Assumption 1 has been used to get the second identity, (7) for the first inequality, (8) again for the third equation and (10) for the last identity.

Remark 1. A key step for the utilization of the previous result is the derivation of the desired trajectories x_* and their corresponding control signals u_* , which satisfy (2). As shown in the examples below this may prove to be a very complicated task and some approximations may be needed to derive them. Indeed, it is shown in Olm et al. (2011) that even for the simple boost converter this task involves the search of a stable solution of an Abel ordinary differential equation, which is known to be highly sensitive to initial conditions.

4. A PI GLOBAL TRACKING CONTROLLER

From Lemma 1 the next proposition follows immediately.

Proposition 1. Consider the system (1) verifying Assumption 1 and an admissible trajectory x_* in closed loop with the PI controller

$$\begin{aligned}
\dot{z} &= -y \\
u &= -K_p y + K_i z + u_*
\end{aligned} \tag{14}$$

with output (10), (11) and $K_p = K_p^\top > 0$, $K_i = K_i^\top > 0$. For all initial conditions $(x(0), z(0)) \in \mathbb{R}^n \times \mathbb{R}^m$ the trajectories of the closed-loop system are bounded and

$$\lim_{t \rightarrow \infty} y_a(t) = 0, \tag{15}$$

where the augmented output $y_a : \mathbb{R}_+ \rightarrow \mathbb{R}^{m+n}$ is defined as

$$y_a := \begin{bmatrix} \mathcal{C}(x_*) \\ Q^{\frac{1}{2}} \end{bmatrix} \tilde{x},$$

with $Q^{\frac{1}{2}}$ the square root of Q given in (9). Moreover, if

$$\text{rank} \begin{bmatrix} \mathcal{C}(x_*) \\ Q^{\frac{1}{2}} \end{bmatrix} = n, \tag{16}$$

then state global tracking is achieved, i.e., (5) holds.

Proof. Notice that the PI controller (14) is equivalent to

$$\begin{aligned}
\tilde{u} &= -K_p y + K_i z \\
\dot{z} &= -y.
\end{aligned}$$

Propose the following radially unbounded Lyapunov function candidate

$$W(\tilde{x}, z) := V(\tilde{x}) + \frac{1}{2} z^\top K_i z,$$

whose time derivative is

$$\begin{aligned}
\dot{W} &= -\tilde{x}^\top Q \tilde{x} + y^\top \tilde{u} - z^\top K_i y \\
&= -\tilde{x}^\top Q \tilde{x} - y^\top K_p y \\
&\leq -\lambda_{\min}\{K_p\} |y|^2 - |Q^{\frac{1}{2}} \tilde{x}|^2 \leq 0
\end{aligned}$$

From here we conclude that the system state $z, \tilde{x} \in \mathcal{L}_\infty$ and $y, Q^{\frac{1}{2}} \tilde{x} \in \mathcal{L}_2$, consequently $y_a \in \mathcal{L}_2$. To conclude that $y_a(t) \rightarrow 0$ it suffices, invoking Tao (1997), to prove that $\dot{y}_a \in \mathcal{L}_\infty$. Towards this end, we first notice that $\tilde{x}, x_* \in \mathcal{L}_\infty$ implies $x \in \mathcal{L}_\infty$ and, this in its turn, implies from (10) $y \in \mathcal{L}_\infty$. Now, $y, z, u_* \in \mathcal{L}_\infty$ implies, from (14), $u \in \mathcal{L}_\infty$. That implies, from (13), $\dot{x} \in \mathcal{L}_\infty$. Now, compute

$$\dot{y} = \begin{bmatrix} \dot{x}_*^\top B_1^\top \\ \vdots \\ \dot{x}_*^\top B_m^\top \end{bmatrix} P \tilde{x} + \begin{bmatrix} x_*^\top B_1^\top \\ \vdots \\ x_*^\top B_m^\top \end{bmatrix} P \dot{\tilde{x}}, \tag{17}$$

which is bounded because $\dot{x}_* \in \mathcal{L}_\infty$.

The proof of global state tracking follows noting that $y_a(t) \rightarrow 0$ ensures (5) if the rank condition (16) holds.

Remark 2. Notice that the matrix \mathcal{C} depends on the reference trajectory. Therefore, the rank condition (16) identifies a class of trajectories for which global tracking is ensured.

Remark 3. Condition (16) is sufficient, but not necessary for state convergence. Indeed, as shown in van der Schaft (2000), global tracking is guaranteed if y_a is a detectable output for the closed-loop system. That is, if the following implication holds

$$y_a(t) \equiv 0 \implies \lim_{t \rightarrow \infty} [x(t) - x_*(t)] = 0.$$

5. APPLICATION TO POWER FACTOR COMPENSATION IN A BOOST CONVERTER

5.1 Model and Problem Formulation

The following scenario corresponds to the PFC of an AC–DC boost converter. Assuming linear loads and sinusoidal steady-state regime it is well-known that the power factor is optimized when the line current is in phase with line voltage.² Hence, the problem can be recast as tracking problem that fits the theoretical framework given in the previous sections. An additional requirement imposed to the PFC is to reduce the distortion in the current, which can also distort the line voltage. A standard measure to assess this property is the Total Harmonic Distortion (THD) index.

The interleaved AC–DC boost is one of the most popular PFC topologies in real applications. The idea of this topology is to incorporate N branches with their own switch, each of whom admitting the control signal shifted by $\frac{2\pi}{N}$. When assuming parasitic parameters such as the voltage drop or losses in the diodes, a typical form of a two branches converter is depicted in Fig. 1. Since these parameters are usually small, they will be neglected. Hence, from Fig. 1, $R_{DS}, R_D, R_L = 0$. Under this consideration, the model equations are

² See García-Canseco et al. (2007) for the case of nonlinear loads and non-sinusoidal regime.

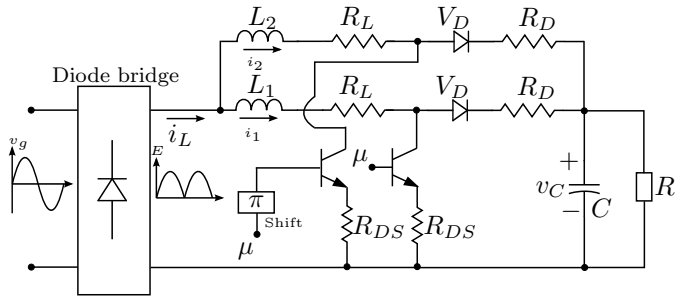


Fig. 1. Boost converter circuit

$$\begin{aligned}\dot{i}_1 &= -\frac{1}{L_1}(1-\mu')v_C + \frac{E}{L_1} \\ \dot{i}_2 &= -\frac{1}{L_2}(1-\mu')v_C + \frac{E}{L_2} \\ \dot{v}_C &= \frac{1}{C}(1-\mu')i_1 + \frac{1}{C}(1-\mu')i_2 - \frac{1}{RC}v_C,\end{aligned}\quad (18)$$

where E is the rectified AC voltage L_1, L_2, C, R are the boost inductance, capacitance and load resistance, respectively, and $\mu = 1 - \mu'$ is the duty cycle of the switch. If it is assumed that $L_1 = L_2 = \frac{L}{2}$, it follows that $i_1 = i_2 = \frac{1}{2}i_L$ and, according to Kirchhoff's law, $i_L = i_1 + i_2$ (see Fig. 1). Then, using the latter and defining $x := [i_L \ v_C]^\top$ and $u = 1 - \mu'$, equations (18) can be expressed as

$$\begin{aligned}\dot{x}_1 &= -\frac{2}{L}ux_2 + \frac{2}{L}E \\ \dot{x}_2 &= \frac{1}{C}ux_1 - \frac{1}{RC}x_2,\end{aligned}\quad (19)$$

Clearly, the system (19) can be written in the form (1) with the following definitions

$$A = \begin{bmatrix} 0 & 0 \\ 0 & -\frac{1}{RC} \end{bmatrix}, \quad d = \begin{bmatrix} \frac{2E}{L} \\ 0 \end{bmatrix}, \quad B = \begin{bmatrix} 0 & -\frac{2}{L} \\ \frac{1}{C} & 0 \end{bmatrix}.$$

A matrix P that verifies the conditions of Assumption 1 is

$$P = \begin{bmatrix} \frac{L}{2} & 0 \\ 0 & C \end{bmatrix}, \quad (20)$$

then

$$Q = \begin{bmatrix} 0 & 0 \\ 0 & \frac{1}{R} \end{bmatrix}. \quad (21)$$

Furthermore, the passive output y is

$$\begin{aligned}y &= x_\star^\top B^\top x \\ &= x_{1\star}x_2 - x_{2\star}x_1.\end{aligned}\quad (22)$$

Now, convergence of the state is tested by means of the matrix

$$\begin{bmatrix} \mathcal{C}(x_\star) \\ Q^{\frac{1}{2}} \end{bmatrix} = \begin{bmatrix} -x_{2\star} & x_{1\star} \\ 0 & 0 \\ 0 & \frac{1}{\sqrt{R}} \end{bmatrix},$$

which satisfies the rank condition (16), provided x_2^* is bounded away from zero, which is consistent with the operating mode of the boost, i.e., $x_2 > 0$.

Reference signals $x_{2\star}$, $x_{1\star}$ and u_\star are derived below.

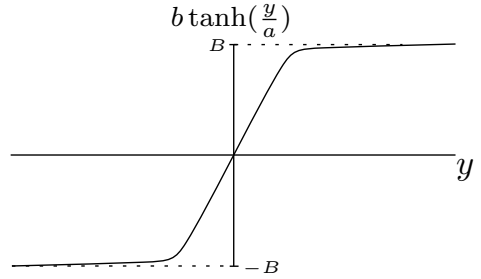


Fig. 2. Function $B \tanh(\frac{y}{A})$

5.2 Generation of references

It is assumed that the dynamics of the output voltage x_2 is slower respect to that of the current x_1 . The objective of control is to drive x to x_\star in such a way that

- (1) $x_{1\star} \propto E$ (Power Factor Correction)
- (2) $x_{1\star} \propto \frac{1}{E_{RMS}}$.
- (3) $x_{2\star}$ is a desired output voltage.

Then, the resulting reference for the inductor current is shown in the following equation:

$$x_{1\star} = \frac{E\phi}{(E_{RMS})^2} \quad (23)$$

where ϕ is the output of a linear compensator $G_{cv}(s)$ whose input is the voltage error and E_{RMS} is the RMS value of the rectified AC voltage. The design of the compensator $G_{cv}(s)$ is based on the perturbation and linearization technique applied in the loss-free resistor (LFR) boost model Erickson and Maksimovic (2001). This results in equivalent small-signal circuit for the design of the following transfer function Ridley (1989)

$$\frac{\hat{x}_2(s)}{\hat{\phi}(s)} = \frac{P_{av}}{sCX_2\Phi}, \quad (24)$$

where $\hat{x}_2(s)$ and X_2 are respectively the Laplace small signal of x_2 and its DC output voltage, also $\hat{\phi}(s)$ and Φ are respectively the Laplace small signal of ϕ and its DC compensator output control signal, P_{av} is the average rectifier power and C is the boost capacitance. This transfer function neglects the complicating effects of high-frequency switching ripple, and is valid for control variations at frequencies sufficiently lower than the AC line frequency. Ultimately, the linear compensator $G_{cv}(s)$ consists of a PI with anti-windup technique Erickson and Maksimovic (2001). The output voltage controller must have sufficiently small gain at frequency and minimize the negative effect of the Right Half Plane (RHP) zero. Hence its bandwidth must be low. As a rule of thumb, setting the overall control loop bandwidth to a third of the RHP zero is enough to provide the closed loop stability. It requires, however, a compromise in the control performance. Erickson and Maksimovic (2001).

The design of the controller is concluded with the calculation of u_\star . Thus, from the first equation of (19)

$$u_\star = \frac{2E - L\dot{x}_{1\star}}{2x_{2\star}}. \quad (25)$$

Table 1.

Indexes	PF	THD
Proportional	96.7%	23.2%
Hyperbolic Tangent	98.2%	21.1%

5.3 The Controller

In summary, the resulting controller equations for the PFC AC-DC Boost Converter are the following.

$$\begin{aligned} \dot{z} &= -y \\ u &= -K_p y + K_i z + u_* \\ y &= x_{1*} x_2 - x_{2*} x_1 \\ u_* &= \frac{2E - L\dot{x}_{1*}}{2x_{2*}} \\ x_{1*} &= \frac{E\phi}{(E_{RMS})^2} \end{aligned} \quad (26)$$

where ϕ is the output of the anti-windup PI and x_{2*} is the desired DC output voltage.

Remark 4. It is customary to implement a PI controller with changing gains. Usually nonlinear functions as the $\tanh(\cdot)$ are introduced. In this case, a modification in the second equation of (26) leads to

$$u = -b \tanh\left(\frac{y}{a}\right) + K_i z + u_* \quad (27)$$

where a and b are free parameters to be adjusted. A typical shape of function $b \tanh(\cdot)$ is depicted in Fig. 2. As a matter of fact this change does not compromise the stability of the system. It comes down to the fact that the function $\tanh(y)$ can be considered as the product $k_p(y)y$ where $k_p(y)$ is scalar function taking nonnegative bounded values except at $y = 0$ where it is zero. A practical comparison between controller (26) and its modification will be shown in the sequel.

5.4 Simulations and Experimental Results

The interleaved Boost converter was simulated under the following considerations: the output voltage reference $V_{ref} = 15V$, the PWM frequency $PWM_{Freq} = 100KHz$ and the input voltage $v_g = 9|\sin(2\pi f_{line})|$ where $f_{line} = 50Hz$.

Boost inductance, capacitance and load values are respectively: $L = 56\mu H$, $C = 3047\mu F$, $R = 22\Omega$. The gain for the compensator $G_{cv}(s)$ and for the passivity PI have been respectively set to $k_{p(comp)} = 0.011$, $k_{i(comp)} = 0.03$ and $K_p = 0.013$, $K_i = 0.0001$ whereas the hyperbolic tangent parameters are $a = 55$ and $b = 0.25$.

Figure 3 shows the trend of the inductor current i_L and of the input voltage v_g in an interval time during the steady state: it is clear that the current i_L (the blue line) and input voltage v_g (the red line) have the same shape, except in the instants in which the value of v_g is low driving the boost to the Discontinuous Conduction Mode (DCM). Also performance indexes, displayed in Table 1, confirm that the control reaches the main objective and suggest the use of the hyperbolic tangent instead of PI because of its slightly better performances. Figure 4 shows the trends of the output voltage v_C . Its reference value, namely $15V$, is completely reached in $0.8s$. Finally, Figure 5 shows v_C

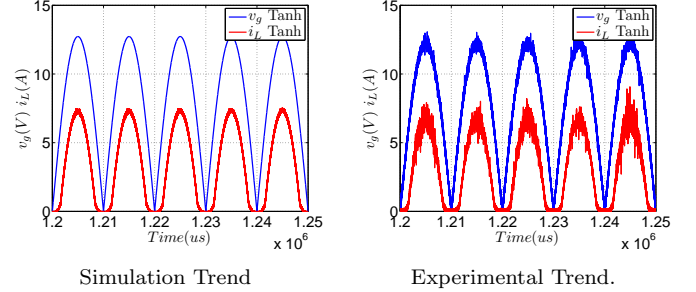


Fig. 3. Inductor Current i_L and Input Voltage v_g Trend.

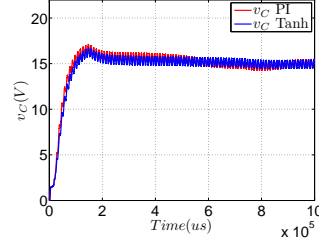


Fig. 4. Output Voltage v_C Transient. Comparison between (26) and (27)

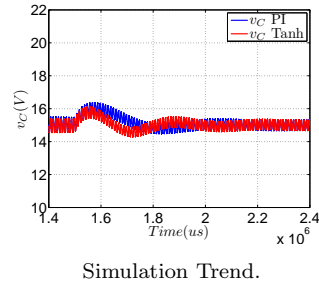


Fig. 5. Output Voltage v_C Trend with a load change of 30%. Comparison between (26) and (27)

trend after a load change of 30% which occurs at $1.5s$. As it can be seen, after an initial transient the system is stabilized again around the reference value. Even if the gains can be tuned to slightly change the performances achieved, in general it could be stated that the hyperbolic tangent function has better performances in the steady state, both as regards the disturbance response and the performance indicators (PF and THD).

6. PHASE INDEPENDENT CONTROL FOR MODULAR MULTILEVEL CONVERTER

6.1 Model and Problem Formulation

The MMC introduced by Prof. Marquart in Glinka and Marquardt (2003) has several advantages with respect to its predecessors, such as its high modularity, scalability and lower losses. It seems to be one of the most promising converters for bulk power transmission via HVDC links Ahmed et al. (2011).

Nonetheless, controlling the MMC is no simple task. Several efforts have been oriented to propose suitable mathematical dynamical models Antonopoulos et al. (2009);

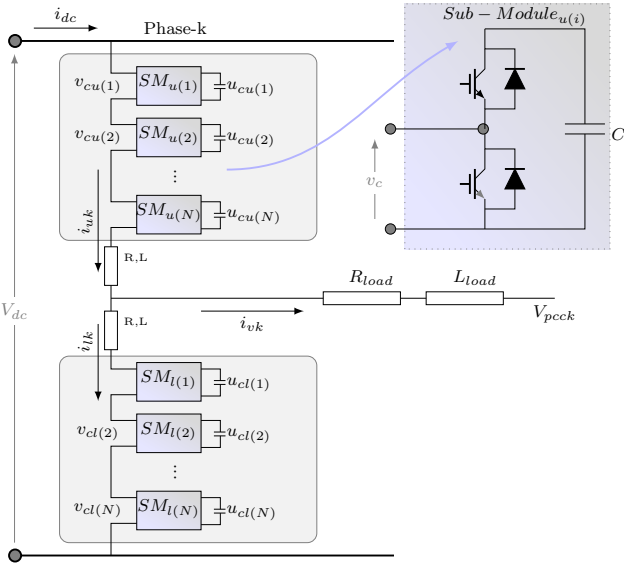


Fig. 6. MMC Topology

Harnefors et al. (2012), and control strategies for the converter under balanced operation. Some of the proposed control strategies have been implemented in *dqo* rotating reference frame such as Tu et al. (2011); Bergna et al. (2012). Nonetheless, it seems to be getting clear that there are significant disadvantages in applying *dqo*-based control schemes for the control of the MMC differential currents since they do not facilitate complete phase-independent control of the converter state variables, hence the MMC potential will not be fully exploited Bergna et al. (2013). To overcome this drawback it is necessary to formulate the control problem in the *abc* frame—in which the MMC is controlled independently per phase—resulting in a tracking problem instead of a regulation one.

The MMC converter studied in the paper is shown in Fig. 6. To obtain its mathematical model four state variables have been considered: 1) The differential or circulating current of the MMC i_{diff} , 2) the grid or load current i_v , 3) the sum between the upper and lower capacitor voltages $u_{C\Sigma} := u_{CU} + u_{CL}$, and 4) the difference between them $u_{C\Delta} := u_{CU} - u_{CL}$. This yields the model

$$\begin{aligned}\dot{i}_{diff} &= -\frac{R}{L}i_{diff} - \frac{1}{4L}u_{C\Sigma}u_{\Sigma} - \frac{1}{4L}u_{C\Delta}u_{\Delta} + \frac{v_{dc}}{2L} \\ i_v &= -\frac{R'}{L'}i_v - \frac{1}{4L'}u_{C\Delta}u_{\Sigma} - \frac{1}{4L'}u_{C\Sigma}u_{\Delta} - \frac{V_{pcc}}{L'} \\ \dot{u}_{C\Sigma} &= \frac{1}{C'}i_{diff}u_{\Sigma} + \frac{1}{2C'}i_vu_{\Delta} \\ \dot{u}_{C\Delta} &= \frac{1}{2C'}i_vu_{\Sigma} + \frac{1}{C'}i_{diff}u_{\Delta},\end{aligned}\quad (28)$$

where the control signals are u_{Σ} and u_{Δ} and the other signals and constants can be identified from Fig. 6 (Refer to Harnefors et al. (2012); Antonopoulos et al. (2009) for more details on the model). Also, henceforth $V_{pcc} = 0$ since the system here studied is not considered to be connected to grid. In addition, notation for the equivalent capacitance $C' := C/N$, the equivalent inductance $L' := L/2 + L_{load}$ and resistance $R' := R/2 + R_{load}$ has been introduced for the sake of clarity. Defining $x := [i_{diff} \ i_v \ u_{C\Sigma} \ u_{C\Delta}]^{\top}$ and $u := [u_{\Sigma} \ u_{\Delta}]^{\top}$, the system can

be written in the form (1) with:

$$A = \begin{bmatrix} -\frac{R}{L} & 0 & 0 & 0 \\ 0 & -\frac{R'}{L'} & 0 & 0 \\ 0 & 0 & 0 & 0 \\ 0 & 0 & 0 & 0 \end{bmatrix}, d = \begin{bmatrix} \frac{v_{dc}}{2L} \\ 0 \\ 0 \\ 0 \end{bmatrix},$$

$$B_1 = \begin{bmatrix} 0 & 0 & \frac{-1}{4L} & 0 \\ 0 & 0 & 0 & \frac{-1}{4L'} \\ \frac{1}{C'} & 0 & 0 & 0 \\ 0 & \frac{1}{2C'} & 0 & 0 \end{bmatrix}, B_2 = \begin{bmatrix} 0 & 0 & 0 & \frac{-1}{4L} \\ 0 & 0 & \frac{-1}{4L'} & 0 \\ 0 & \frac{1}{2C'} & 0 & 0 \\ \frac{1}{C'} & 0 & 0 & 0 \end{bmatrix}.$$

Therefore, the matrix P satisfying Assumption (1) is

$$P = \begin{bmatrix} 2L & 0 & 0 & 0 \\ 0 & L' & 0 & 0 \\ 0 & 0 & \frac{C'}{2} & 0 \\ 0 & 0 & 0 & \frac{C'}{2} \end{bmatrix}.$$

The passive output defined in (10) is

$$\begin{aligned}y &= \begin{bmatrix} x_{1\star}^{\top} B_1^{\top} \\ x_{2\star}^{\top} B_2^{\top} \end{bmatrix} Px \\ &= \frac{1}{2} \begin{bmatrix} x_{1\star}x_3 - x_{1\star}x_3 + \frac{1}{2}x_{2\star}x_4 - \frac{1}{2}x_{2\star}x_4 \\ x_{1\star}x_4 - x_{1\star}x_4 + \frac{1}{2}x_{2\star}x_3 - \frac{1}{2}x_{2\star}x_3 \end{bmatrix}.\end{aligned}\quad (29)$$

The convergence condition (16) imposes that the rank of the matrix

$$\begin{bmatrix} \mathcal{C} \\ Q^{\frac{1}{2}} \end{bmatrix} = \begin{bmatrix} -\frac{1}{2}x_{3\star} & -\frac{1}{4}x_{4\star} & \frac{1}{2}x_{1\star} & \frac{1}{4}x_{2\star} \\ -\frac{1}{2}x_{4\star} & -\frac{1}{4}x_{3\star} & \frac{1}{4}x_{2\star} & \frac{1}{2}x_{1\star} \\ \sqrt{2R} & 0 & 0 & 0 \\ 0 & \sqrt{R'} & 0 & 0 \\ 0 & 0 & 0 & 0 \\ 0 & 0 & 0 & 0 \end{bmatrix}$$

should be full. This is clearly the case if

$$x_{1\star}^2 - \frac{1}{4}x_{2\star}^2 \neq 0,\quad (30)$$

6.2 Generation of references

As indicated in Remark 1 obtaining the exact expressions for the desired trajectories x_{\star} and their corresponding control signals u_{\star} that satisfy (2) is a very complicated task. Therefore, in this subsection several practical considerations have been made, which are widely adopted in the power electronics community, to approximate their solution.

The reference equilibrium point for the grid current is imposed based on the desired voltage reference of the load. For the system under study with no grid connection (i.e., $V_{pcc} = 0$) such reference is found by means of simple phasor calculations; i.e., by dividing the internal e.m.f. voltage of the MMC ($e_{v\star} = |e_{v\star}|e^{j\omega t}$) by the equivalent impedance ($Z' = R' + jwL'$).

$$x_{2\star} = \frac{|e_{v\star}|}{\sqrt{R'^2 + (\omega L')^2}} \sin \left(\omega t - \tan^{-1} \left(\frac{\omega L'}{R'} \right) \right)\quad (31)$$

where $e_{v\star}$ is the sinusoidal voltage that one wishes to apply to the load, with an amplitude that can vary from 0 to $\frac{V_{dc}}{2}$. The differential or circulating current reference $x_{1\star}$ is estimated by assuming low converter losses; hence, the mean value of the input ac power $|P_{ac}| = |e_{v\star}x_{2\star}|$ is approximately equal to the mean value of the power at the

dc terminals of the MMC $|P_{dc}| = V_{dc}x_{1\star}$. Thus, $x_{1\star}$ can be expressed as

$$x_{1\star} \approx \frac{|e_{v\star}x_{2\star}|}{V_{dc}}. \quad (32)$$

Since $x_{1\star}$ is constant in this case, the voltage that drives it may be expressed simply by $u_{diff\star} = Rx_{1\star}$.

Also, it is possible to calculate the fluctuations of the sum $w_{\Sigma\star}$ and difference $w_{\Delta\star}$ of the capacitive energy stored between the upper and lower arms of the MMC (see Harnefors et al. (2012) for more details on such equations). Thus,

$$\begin{aligned}\Delta w_{\Sigma\star} &= \int_0^t (-e_{v\star}x_{2\star} + (V_{dc} - 2u_{diff\star})x_{1\star}) dt \\ \Delta w_{\Delta\star} &= \int_0^t \left(\frac{x_{2\star}}{2}(V_{dc} - 2u_{diff\star}) - 2e_{v\star}x_{1\star} \right) dt\end{aligned}\quad (33)$$

Remark 5. A high-pass filter is needed for the term that is being integrated in equation (33) to leave out the power error caused by neglecting assuming no losses in the converter (32).

The average value of $w_{\Sigma\star}$ and $w_{\Delta\star}$ is given as a reference from the user; typically, $W_{\Sigma\phi\star} = \frac{C}{N}V_{dc}^2$, and $W_{\Delta\phi\star} = 0$. Using the energy estimation, it is now possible to calculate the upper and lower arm voltages.

$$\begin{aligned}u_{CU\star} &= \sqrt{\frac{N}{C} [(W_{\Sigma\phi\star} + \Delta w_{\Sigma\star}) + (W_{\Delta\phi\star} + \Delta w_{\Delta\star})]} \\ u_{CL\star} &= \sqrt{\frac{N}{C} [(W_{\Sigma\phi\star} + \Delta w_{\Sigma\star}) - (W_{\Delta\phi\star} + \Delta w_{\Delta\star})]}\end{aligned}\quad (34)$$

The remaining state variables $u_{\Sigma\star}$ and $u_{\Delta\star}$ may now be calculated as

$$\begin{aligned}x_{3\star} &= u_{CU\star} + u_{CL\star} \\ x_{4\star} &= u_{CU\star} - u_{CL\star}\end{aligned}\quad (35)$$

In addition, the upper and lower insertion indexes are calculated by

$$\begin{aligned}n_{u\star} &= \frac{\frac{V_{dc}}{2} - e_{v\star} - u_{diff\star}}{u_{cu\star}} \\ n_{l\star} &= \frac{\frac{V_{dc}}{2} + e_{v\star} - u_{diff\star}}{u_{cl\star}}\end{aligned}\quad (36)$$

Finally, consistent with this methodology, the control at the desired trajectory is defined as:

$$\begin{aligned}u_{1\star} &= n_{u\star} + n_{l\star} \\ u_{2\star} &= n_{uk\star} - n_{l\star}\end{aligned}\quad (37)$$

6.3 The Controller

To summarize, the controller equations are:

$$\begin{aligned}\dot{z} &= -y \\ u &= -K_p y + K_i z + u^* \\ y &= \frac{1}{2} \left[x_{1\star}x_3 - x_1x_{3\star} + \frac{1}{2}x_{2\star}x_4 - \frac{1}{2}x_2x_{4\star} \right] \\ &\quad \left[x_{1\star}x_4 - x_1x_{4\star} + \frac{1}{2}x_{2\star}x_3 - \frac{1}{2}x_2x_{3\star} \right]\end{aligned}$$

with reference variables $x_{2\star}$ defined in (31), $x_{1\star}$ in (32) and $x_{3\star}$, $x_{4\star}$ in (33), (34) and (35). Also, $u_{1\star}$ and $u_{2\star}$ are derived in (37) and (36).

6.4 Simulations and experimental results

The MMC simulation scenario has been set up in Matlab/Simulink using a high efficiency model Gnanarathna

et al. (2011) to test the validity of the control. The considerations are the following: the converter has $2N = 10$ submodules, N in each arm (upper and lower). The input DC voltage is $V_{dc} = 150V$, the reference voltage $e_{v\star}$ has an amplitude of $\frac{V_{dc}}{2}$ and the frequency set to $50Hz$. The frequency of the balancing algorithm Antonopoulos et al. (2009); Harnefors et al. (2012); Glinka and Marquardt (2003) that balances the N capacitor voltages is set to $20kHz$. The internal capacitance, resistance and inductance are respectively set to $C = 3.3mF$, $R = 8\Omega$ and $L = 10mH$. The load resistance and inductance values, respectively, are $R = 6\Omega$ and $L = 20mH$.

The figures presented show the controller performance for both the simulation and implementation scenarios. Figure 7 shows the differential and load current, respectively, i_{diff} and i_v . The grid current tracks with significant accuracy its reference orbit. The differential current and the capacitor voltages achieve good performance; however, they are strongly influenced by high-order harmonic pollution. This is caused by the long switching dead-time requirement of the experimental setup. In Fig. 8 it is shown the values for the upper and lower capacitor voltages u_{CU} and u_{CL} . According to our calculations in the simulations, there is an error of around 3% between these voltages signals and their references. It can be concluded that is a direct consequence of the approximations made in the estimation process. Finally, in Fig. 9 are depicted the $2N$ voltages of the MMC capacitors while fig. 10 shows the output multilevel waveform of the converter.

7. CONCLUSIONS

In this article the trajectory tracking problem for power converters based on passivity foundations has been solved. Because of the use of passivity (of the incremental model) the controller is a simple PI. The stability results are global and hold for all positive definite gains of the PI. In fact, this outcome extends previous results obtained for the regulation case.

The performance of the controller was tested by means of some realistic simulations and experiments for both the boost and the Modular Multilevel Converters models. A future work within this area of research includes the use of observers for partial state feedback and its succeeding application to power converters.

REFERENCES

- Ahmed, N., Haider, A., Van Hertem, D., Zhang, L., and Nee, H.P. (2011). Prospects and challenges of future HVDC SuperGrids with modular multilevel converters. In *Power Electronics and Applications (EPE 2011), Proceedings of the 2011-14th European Conference on*, 1–10.
- Antonopoulos, A., Angquist, L., and Nee, H.P. (2009). On dynamics and voltage control of the Modular Multilevel Converter. In *Power Electronics and Applications, 2009. EPE '09. 13th European Conference on*, 1–10.
- Bahrman, M. and Johnson, B. (2007). The ABCs of HVDC transmission technologies. *Power and Energy Magazine, IEEE*, 5(2), 32–44.
- Bergna, G., Berne, E., Egrot, P., Lefranc, P., Amir, A., Vannier, J., and Molinas, M. (2012). An energy-based

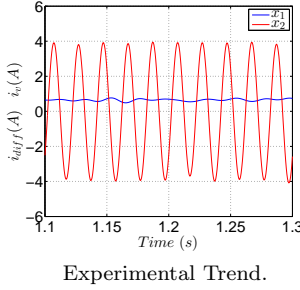
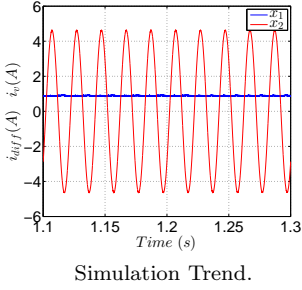


Fig. 7. Differential and Load currents.

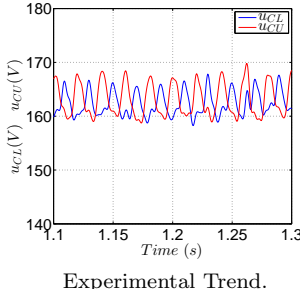
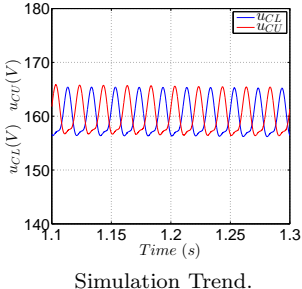


Fig. 8. Upper and Lower capacitor voltages.

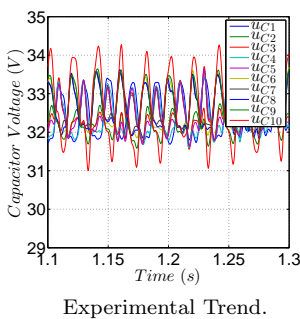
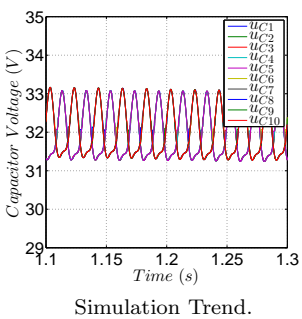


Fig. 9. Individual capacitor voltages.

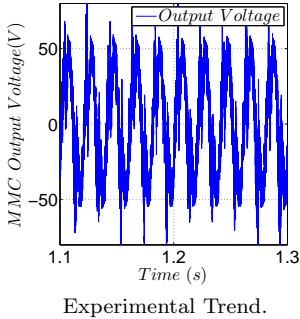
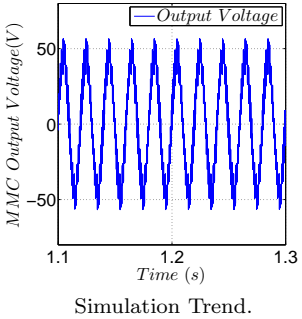


Fig. 10. Multilevel output waveform applied to the load.

controller for HVDC Modular Multilevel Converter in Decoupled Double Synchronous Reference Frame for Voltage Oscillations Reduction. *Industrial Electronics, IEEE Transactions on*, PP(99), 1.

Bergna, G., Garces, A., Berne, E., Egrot, P., Arzande, A., Vannier, J.C., and Molinas, M. (2013). A generalized Power Control Approach in ABC Frame for Modular Multilevel Converter HVDC links based on Mathematical Optimization. *Power Delivery, IEEE Transactions on*, PP(99), 1–9.

Biel, D., Guinjoan, F., Fossas, E., and Chavarria, J. (2004). Sliding-mode control design of a boost-buck switching converter for AC signal generation. *Circuits and Systems I: Regular Papers, IEEE Transactions on*, 51(8), 1539–1551.

Castaños, F., Jayawardhana, B., Ortega, R., and García-Canseco, E. (2009). Proportional plus integral control for set-point regulation of a class of nonlinear RLC circuits. *Circuits, Systems and Signal Processing*, 28(4), 609–623.

Cimini, G., Corradini, M.L., Ippoliti, G., Orlando, G., and Pirro, M. (2013). Passivity-based PFC for interleaved Boost converter of PMSM drives. In *Adaptation and Learning in Control and Signal Processing*, volume 11, 128–133.

Cisneros, R., Pirro, M., Berna, G., Ortega, R., Ippoliti, G., and Molinas, M. (2015). Global tracking Passivity-based PI control of bilinear systems: An application to the boost and modular multilevel converters (*accepted*). In *1st Conference on Modelling, Identification and Control of Nonlinear Systems (MICNON-2015)*.

Elliott, D. (2009). *Bilinear control systems: Matrices in action*. Applied mathematics science. Springer.

Erickson, R. and Maksimovic, D. (2001). *Fundamentals of Power Electronics*. Springer.

Fadili, A.E., Giri, F., Magri, A.E., Lajouad, R., and Chaoui, F. (2012). Towards a global control strategy for induction motor: Speed regulation, flux optimization and power factor correction. *International Journal of Electrical Power & Energy Systems*, 43(1), 230 – 244.

Flourentzou, N., Agelidis, V., and Demetriadis, G. (2009). Vsc-based HVDC power transmission systems: An overview. *Power Electronics, IEEE Transactions on*, 24(3), 592–602.

Fossas, E. and Olm, J.M. (1994). Generation of signals in a buck converter with sliding mode control. In *Circuits and Systems, 1994. ISCAS '94., 1994 IEEE International Symposium on*, volume 6, 157–160.

Fossas, E. and Olm, J.M. (2009). A functional iterative approach to the tracking control of nonminimum phase switched power converters. *Mathematics of Control, Signals, and Systems*, 21(3).

García-Canseco, E., Gríñó, R., Ortega, R., Salich, M., and Stankovic, A. (2007). Power factor compensation of electrical circuits: The nonlinear non-sinusoidal case. *IEEE Control Systems Magazine* vol. 27 chap. 4, 46–59.

Glinka, M. and Marquardt, R. (2003). A new AC/AC-multilevel converter family applied to a single-phase converter. In *Power Electronics and Drive Systems, 2003. PEDS 2003. The Fifth International Conference on*, volume 1, 16 – 23 Vol.1.

Gnanarathna, U., Gole, A., and Jayasinghe, R. (2011). Efficient Modeling of Modular Multilevel HVDC Converters (MMC) on electromagnetic transient simulation programs. *Power Delivery, IEEE Transactions on*, 26(1), 316 – 324.

Harnefors, L., Antonopoulos, A., Norrga, S., Angquist, L., and Nee, H. (2012). Dynamic analysis of Modular Multilevel Converters. *Industrial Electronics, IEEE Transactions on*, PP(99), 1.

Hernandez-Gomez, M., Ortega, R., Lamnabhi-Lagarrigue, F., and Escobar, G. (2010). Adaptive PI stabilization of switched power converters. *Control Systems Technology*,

- IEEE Transactions on*, 18(3), 688–698.
- Hussain, E.K., Bingham, C., and Stone, D. (2011). Grid connected PVs amp & wind turbine with a wide range of reactive power control and active filter capability. In *Innovative Smart Grid Technologies (ISGT Europe), 2011 2nd IEEE PES International Conference and Exhibition on*, 1–6.
- Jayawardhana, B., Ortega, R., García-Canseco, E., and Castaños, F. (2007). Passivity of nonlinear incremental systems: Application to PI stabilization of nonlinear RLC circuits. *Systems & Control Letters*, 56(910), 618–622.
- Mather, B. and Maksimovic, D. (2011). A simple digital Power–Factor correction rectifier controller. *Power Electronics, IEEE Transactions on*, 26(1), 9–19.
- Meza, C., Biel, D., Jeltsema, D., and Scherpen, J.M.A. (2012). Lyapunov-Based Control scheme for single-phase grid-connected PV Central Inverters. *Control Systems Technology, IEEE Transactions on*, 20(2), 520–529.
- Meza, C., Jeltsema, D., Scherpen, J.M., and Biel, D. (2008). Passive P-control of a grid-connected photovoltaic inverter. In *17th World Congress, Preceedings of the*, volume 21, 3808–3812.
- Mohler, R. (2003). *Encyclopedia of Physical Science and Technology*. Academic Press, New York, third edition edition.
- Olm, J.M., Ros-Oton, X., and Shtessel, Y.B. (2011). Stable inversion of abel equations: Application to tracking control in DC-DC nonminimum phase boost converters. *Automatica*, 47(1), 221–226.
- Ridley, R. (1989). Average small-signal analysis of the boost Power Factor Correction circuit. In *Proceedings of the Virginia Power Electronics Center Seminar*, 108–120.
- Sanders, S.R. and Verghese, G.C. (1992). Lyapunov-based control for switched power converters. *Power Electronics, IEEE Transactions on*, 7(1), 17–24.
- Tao, G. (1997). A simple alternative to the Barbalat lemma. *Automatic Control, IEEE Transactions on*, 42(5), 698.
- Tu, Q., Xu, Z., and Xu, L. (2011). Reduced Switching-Frequency Modulation and Circulating Current Suppression for Modular Multilevel Converters. *Power Delivery, IEEE Transactions on*, 26(3), 2009 –2017.
- van der Schaft, A. (2000). *L₂-Gain and passivity techniques in nonlinear control*. Communications and Control Engineering Series. Springer-Verlag.
- Zonetti, D., Ortega, R., and Benchaib, A. (2014). A globally asymptotically stable decentralized PI controller for multi-terminal high-voltage dc transmission systems. In *Control Conference (ECC), 2014 European*, 1397–1403.